

See discussions, stats, and author profiles for this publication at: <https://www.researchgate.net/publication/323780357>

# A Step-by-Step Tutorial for a Motor Imagery-Based BCI

Chapter · January 2018

CITATIONS

12

READS

8,452

4 authors, including:



**Hohyun Cho**

Washington University in St. Louis

43 PUBLICATIONS 751 CITATIONS

[SEE PROFILE](#)



**Minkyu Ahn**

Handong Global University

60 PUBLICATIONS 1,159 CITATIONS

[SEE PROFILE](#)



**Sung Chan Jun**

Gwangju Institute of Science and Technology

160 PUBLICATIONS 2,489 CITATIONS

[SEE PROFILE](#)

Some of the authors of this publication are also working on these related projects:



Stereoscopic 3D images research using EEG/MEG [View project](#)



Multi-brain Interaction [View project](#)

---

# 23 A Step-by-Step Tutorial for a Motor Imagery–Based BCI

*Hohyun Cho, Minkyu Ahn, Moonyoung Kwon,  
and Sung Chan Jun*

## CONTENTS

23.1	Introduction: Motor Imagery–Based BCI.....	446
23.2	Training Session .....	446
23.2.1	Recording MI Data .....	446
23.2.1.1	Recording Device and Software .....	446
23.2.1.2	Subjects .....	447
23.2.1.3	Environment.....	447
23.2.1.4	Experimental Paradigm .....	447
23.2.1.5	MI Instructions .....	449
23.2.1.6	Questionnaire.....	449
23.2.1.7	Discussions.....	449
23.2.2	Training Algorithms and Offline Analysis.....	451
23.2.2.1	Preprocessing .....	451
23.2.2.3	Feature Extraction.....	453
23.2.2.4	Classification.....	454
23.2.2.5	Discussion .....	456
23.3	Testing Session.....	456
23.3.1	Online Experiment .....	456
23.3.2	Discussion .....	457
23.4	Summary .....	458
	Acknowledgments.....	458
	References.....	458

## Abstract

Motor imagery (MI)–based brain–computer interface (BCI) is one of the standard concepts of BCI, in that the user can generate induced activity from motor cortex by imagining motor movements without any limb movement or external stimulus. In this chapter, we present a step-by-step tutorial on MI BCI and discuss the issues involved in each step. We describe detailed examples of our MI experiment with a general procedure from training session to testing session. In training session, we introduce and discuss recording devices and software, experimental settings, collecting MI data and questionnaires, offline analysis for inhibition of somatosensory rhythm, and training simple machine learning algorithms, including common spatial patterns and Fisher’s linear discriminant analysis. Next, we introduce basic procedures used in the testing session and discuss important issues including session variabilities of electroencephalogram signal and information transfer rate. Last, we summarize the tutorial and list the challenging issues that remain in MI BCI.

## 23.1 INTRODUCTION: MOTOR IMAGERY–BASED BCI

Motor imagery (MI) brain–computer interface (BCI) employs the user’s endogenous brain activity in the absence of any external stimuli (Pfurtscheller and Da Silva 1999; Ramoser et al. 2000; Schalk et al. 2004; Wolpaw and Wolpaw 2012; Wolpaw et al. 1991). A standard concept in BCI is the translation of the user’s intention via mental imagination of motor movement, which serves an interface through which to communicate the user’s intention without limb movement. The most representative application of MI BCI is for neurorehabilitation, and researchers have reported that repetitive MI can have positive effects in such rehabilitation (Mattia et al. 2016; Pichiorri et al. 2015). Thus, MI BCI remains a fascinating topic, although it already has been investigated for approximately 20 years.

Similar to other BCI paradigms, the MI BCI paradigm entails training and testing sessions. In the training session, the experimenter collects each user’s MI data, does feature extraction with them, and makes classification algorithms through the data collected. Thus, it is very important to collect highly informative MI data, as they may provide an easier way to train algorithms. If the data contain many artifacts, then they may require preprocessing techniques that are more complex to remove or reduce any unwanted effects of the artifacts. During the testing session, algorithms already trained are applied to new MI data for classification on a real-time basis. Minimizing the psychological and environmental differences between training and testing sessions is also of significant importance, as trained algorithms do not work properly in the testing session because of session-to-session variability in electroencephalograms (EEGs).

In this chapter, we present a step-by-step tutorial on MI BCI. We describe a detailed MI experiment conducted in the BioComputing laboratory and then discuss the issues involved in each step. This tutorial is composed primarily of two sections: training and testing sessions. First, we introduce the way in which to collect high-quality, informative MI data, as well as several feature extraction and classification algorithms, including the common spatial pattern (CSP) and Fisher’s linear discriminant analysis (FLDA). Next, we introduce basic procedures used in the testing session and review briefly existing techniques used to overcome variability between training and testing sessions. Last, we summarize the tutorial and list the challenging issues that remain in MI BCI.

## 23.2 TRAINING SESSION

### 23.2.1 RECORDING MI DATA

Here, we introduce the procedures involved in an MI experiment in the BioComputing laboratory (<https://biocomput.gist.ac.kr>) at Gwangju Institute of Science and Technology (GIST), South Korea. Public access to our data set will be available soon in GigaDB (Cho et al. 2017). At the end of this section, we discuss possible research topics related to recording techniques, subjects, experimental environments, experimental paradigms, MI instruction for subjects, and metadata (questionnaire).

#### 23.2.1.1 Recording Device and Software

As Figure 23.1 shows, we used a 64-channel montage based on the international 10–10 system to record EEG signals at 512-Hz sampling rates. Each subject wore an EEG cap. The EEG device used in this experiment was the Biosemi ActiveTwo system (Amsterdam, Netherlands), which uses a direct current (DC) battery as the power source. The BCI2000 system 3.0.2 (Schalk et al. 2004) was used to collect EEG data and present instructions (left-hand or right-hand MI). Furthermore, we recorded electromyography (EMG) and EEG simultaneously to check actual hand movements. Four EMG electrodes were attached to the flexor digitorum profundus and extensor digitorum on both forearms.

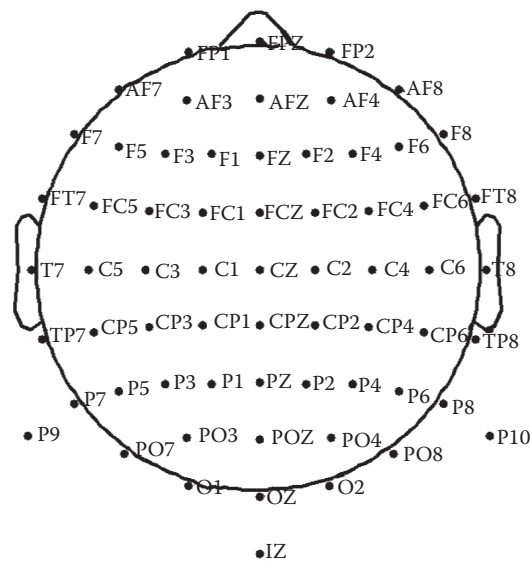


**FIGURE 23.1** EEG channel labeling. (Adapted from Cho, H., Ahn, M., Ahn, S., Kwon, M., and Jun, S.C., 2017. EEG datasets for motor imagery brain computer interface. *GigaScience*. DOI: <https://doi.org/10.1093/gigascience/gix034>. Copyright 2017 by GigaScience.)

### 23.2.1.2 Subjects

We conducted an MI experiment of the left and right hands with 52 subjects (19 females, mean age  $\pm$  SD =  $24.8 \pm 3.86$ ); the Institutional Review Board of GIST (2013-2) approved the experiment. First, we posted a notice on the GIST website. Graduate and undergraduate students, employees, and staff on campus participated in this experiment. All subjects gave informed consent for the researchers to collect information on brain signals and were paid 30,000 Korean Won (approximately \$27) after they participated in the experiment. If a subject's MI data were discriminable—or, if the classification accuracy of left- and right-hand MI was higher than 80%—we paid him or her twice the reward to encourage each subject's concentration.

### 23.2.1.3 Environment

All experiments were conducted in our laboratory during one of four time slots: T1 (9:30–12:00), T2 (12:30–15:00), T3 (15:30–18:00), or T4 (19:00–21:30), as we were interested to know whether BCI performance varied with time. The background noise level was 37–39 decibels because of an air conditioner. The experiments began in August 2011 and ended in September 2011.

### 23.2.1.4 Experimental Paradigm

For each subject, we recorded data for non-task-related and (MI) task-related states, as follows:

**Six types of non-task-related data.** We recorded six types of noise data (eye blinking, eyeball movement up/down, eyeball movement left/right, head movement, jaw clenching, and resting state) for the 52 subjects. Each type of noise was collected twice for 5 s, except for the resting state, which was recorded for 60 s.

**MI experiment.** The experimental design was nearly the same as the Graz MI experiment (Ramoser et al. 2000). Subjects sat in a chair with armrests and watched a monitor. At the beginning of each trial, the monitor showed a black screen with a fixation cross for 2 s; the subject was then prepared to imagine hand movements, and the screen gave a ready signal to the subject. As Figure 23.2 shows, one of two instructions (“left hand” or “right hand”)

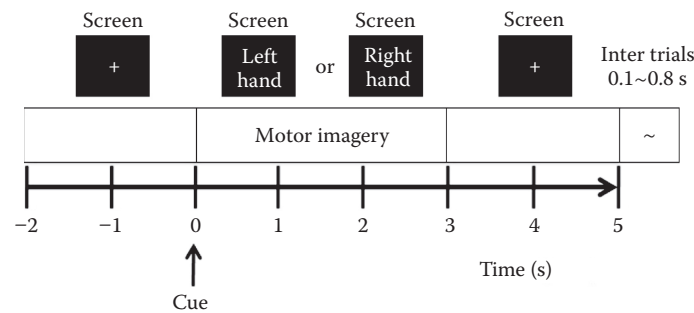


**FIGURE 23.2** Experimental paradigm. One trial of the MI experiment. (Adapted from Cho, H., Ahn, M., Ahn, S., Kwon, M., and Jun, S.C., 2017. EEG datasets for motor imagery brain computer interface. *GigaScience*. DOI: <https://doi.org/10.1093/gigascience/gix034>. Copyright 2017 by GigaScience.)

appeared randomly on the screen for 3 s, and subjects were asked to imagine the hand movement depending on the instruction given. After imagination, when the blank screen appeared, the subject was given a random break of 4.1 to 4.8 s. These processes were repeated 20 times for one class (one run), and five runs were performed. After each run, we calculated the classification accuracy over one run and gave the subject feedback to increase his or her motivation. Between each run, the subjects received a maximum 4-m break depending on their wishes. If interested in a more detailed description of the procedures used to set parameters and configuration, we recommend a mu rhythm BCI tutorial in BCI2000 wiki.

The entire experimental procedure is presented in Table 23.1.

**TABLE 23.1**  
**Experimental Procedure**

Number	Task	Duration (min)
1	Filling out consent form and questionnaire	10
2	EEG electrode placement	20
3	Acquisition of the six types of non-task-related data	2
4	Practicing actual finger movements	3
5	RUN 1	6
6	Filling out questionnaire	4
7	RUN 2	6
8	Filling out questionnaire	4
9	RUN 3	6
10	Filling out questionnaire	4
11	RUN 4	6
12	Filling out questionnaire	4
13	RUN 5	6
14	Filling out questionnaire	4
15	Online experiment	6
16	Digitizing 3D coordinates of EEG electrodes	15
17	Removing electrodes and cleaning laboratory	20
	Sum	126

*Source:* Adapted from Cho, H., Ahn, M., Ahn, S., Kwon, M., and Jun, S.C., 2017. EEG datasets for motor imagery brain computer interface. *GigaScience*. DOI: <https://doi.org/10.1093/gigascience/gix034>. Copyright 2017 by GigaScience.

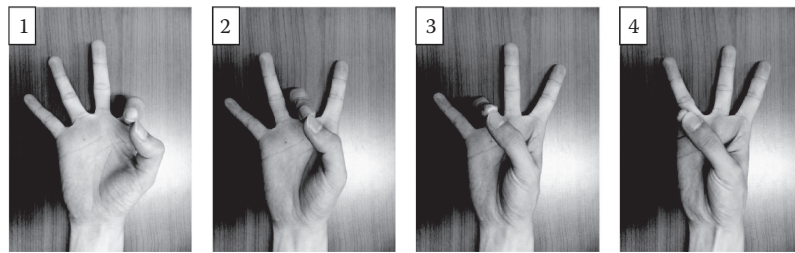


**FIGURE 23.3** Motor imagery instruction. We asked subjects to imagine four actual finger movements: touching each index, middle, ring, and little finger with the thumb within 3 s. Before the MI experiment began, subjects practiced executing the four movements within that time. (Adapted from Cho, H., Ahn, M., Ahn, S., Kwon, M., and Jun, S.C., 2017. EEG datasets for motor imagery brain computer interface. *GigaScience*. DOI: <https://doi.org/10.1093/gigascience/gix034>. Copyright 2017 by GigaScience.)

#### 23.2.1.5 MI Instructions

Before the MI experiment began, we asked each subject to move his or her fingers, beginning with the index finger and proceeding to the little finger (depicted in Figure 23.3) within 3 s after onset. Each subject practiced these actual finger movements before performing the MI experiment. When imagining the movement, we asked subjects to imagine the kinesthetic, rather than the visual experience.

#### 23.2.1.6 Questionnaire

We asked subjects to fill out a questionnaire during the MI experiment, as shown in Table 23.2. Before the MI experiment began, subjects answered 15 questions (questions 101 to 115). After every run, they answered another 10 questions (questions 210 to 219, 220 to 229, etc.). After the MI experiment, we asked the subjects to answer a final set of questions (questions 301 to 304). All numerical responses to the questions were stored in a Microsoft Excel file (Cho et al. 2017).

#### 23.2.1.7 Discussions

In this section, we discuss several points that must be considered in MI BCI experiments, each of which may be an interesting topic for future research.

##### 23.2.1.7.1 Recording Software and Device

It is important to consider the line noise when recording EEG data. A signal power of 50–60 Hz line noise (220 or 110 V, respectively) is much higher than neural oscillation. Although software solutions exist to remove the line noise (e.g., notch filtering), data acquisition hardware that uses DC can reduce the line noise much more than can systems that use alternating current, for example, battery-based hardware. Therefore, we recommend a DC system. Hardware engineers in the BCI field are interested in developing wireless, dry electrode, tripolar concentric electrode, or multimodal EEG to study more accurate and convenient uses of BCI (Ahn et al. 2016; Besio et al. 2006; Cincotti et al. 2006; Nguyen et al. 2016). We believe that the most important issue in software engineering is saving data with correct trigger information and using EEG to study accurate, single-trial–based, and real-time experiments. The literature (Wolpaw and Wolpaw 2012) includes representative types of software for MI experiments: BCI2000 (Schalk et al. 2004), OpenVibe (Renard et al. 2010), and BCILAB (Kothe and Makeig 2013).

##### 23.2.1.7.2 Subjects

The initial goal of research on MI BCIs was to provide a new communication channel for people who are paralyzed completely. For these patients, it is very helpful even to answer “yes” or “no” using left- and right-hand MI. Researchers today tend to study MI for neurorehabilitation of stroke

**TABLE 23.2**  
**Questionnaire for Motor Imagery Experiment**

Questionnaire												
Number	Individual Information				Subject ID:							
101	Time slot (1 = 9:30; 2 = 12:30; 3 = 15:30; 4 = 19:00)											
102	Handedness (0 = left; 1 = right; 2 = both)											
103	Age (number)											
104	Sex (0 = female; 1 = male)											
105	BCI experience (0 = no; number = how many times)											
106	Biofeedback experience (0 = no; number = how many times)											
Before motor imagery experiment												
107.	3. How long did you sleep? (1 = less than 4 h; 2 = 5–6 h; 3 = 6–7 h; 4 = 7–8 h; 5 = more than 8 h)											
108.	4. Did you drink coffee within the past 24 h? (0 = no; number = hours before)											
109.	5. Did you drink alcohol within the past 24 h (0 = no; number = hours before)											
110.	6. Did you smoke within the past 24 h (0 = no; number = hours before)											
111.	7. How do you feel?				Relaxed	1	2	3	4	5	Anxious	
112.					Excited	1	2	3	4	5	Bored	
113.	Physical state				Very good	1	2	3	4	5	Very bad or tired	
114.	Mental state				Very good	1	2	3	4	5	Very bad or tired	
115.	8. BCI performance (accuracy) expected? (%)											
During motor imagery experiment												
Run 1 (after the first run)												
210.	1. Can you continue to the next run? (0 = No; 1 = Yes)											
211.	2. How do you feel?				Relaxed	1	2	3	4	5	Anxious	
212.					Excited	1	2	3	4	5	Bored	
213.	Attention level				High	1	2	3	4	5	Low	
214.	Physical state				Very good	1	2	3	4	5	Very bad or tired	
215.	Mental state				Very good	1	2	3	4	5	Very bad or tired	
216.	3. Have you nodded off (slept awhile) during this run? (0 = no; number = how many times)											
217.	4. Was it easy to imagine finger movements?				Easy	1	2	3	4	5	Difficult	
218.	5. How many trials did you miss? (0 = none; number = how many times)											
219.	6. Was your BCI performance (accuracy) for this run as you expected? (%)											
Run 2 (after the second run)												
220–229	...											
Run 3 (after the third run)												
230–239	...											
Run 4 (after the fourth run)												
240–249	...											
Run 5 (after the fifth run)												
250–259	...											
After the motor imagery experiment												
301.	1. How was this experiment?				Duration	Short	1	2	3	4	5	Long
302.					Procedure	Good	1	2	3	4	5	Bad
303.					Environment	Comfortable	1	2	3	4	5	Uncomfortable
304.	2. Was your overall BCI performance (accuracy) as you expected? (%)											

*Source:* Adapted from Cho, H., Ahn, M., Ahn, S., Kwon, M., and Jun, S.C., 2017. EEG datasets for motor imagery brain computer interface. *GigaScience*. DOI: <https://doi.org/10.1093/gigascience/gix034>. Copyright 2017 by GigaScience.

patients. Clinicians have reported that MI neurofeedback is effective in reestablishing their motor movements immediately after a stroke (Mattia et al. 2016; Pichiorri et al. 2015). For normal subjects, BCI researchers have been interested in performance variation and subject-to-subject transfer to provide subject-independent algorithms (Blankertz et al. 2006; Fazli et al. 2009; Lotte et al. 2009; Reuderink et al. 2011; Samek et al. 2013; Tu and Sun 2012). There is a fraction of BCI-illiterate users in whom it is difficult to detect the mu rhythms from their somatosensory cortex. Identifying and understanding the neurophysiological and psychological characteristics that distinguish high and low performers in MI BCI are also very challenging (Ahn et al. 2013; Ahn and Jun 2015; Blankertz et al. 2010).

#### 23.2.1.7.3 *Environment*

BCI experiments conducted in real time and outside the laboratory are receiving more attention. Most such studies, including this experiment, have been performed in a relatively silent laboratory (37–39 decibels). Ideally, however, we should be able to conduct BCI anywhere. Thus, movement and environmental issues are quite important.

#### 23.2.1.7.4 *Experimental Paradigm*

The classic MI BCI paradigm introduced in this section is simple to follow. To obtain more informative MI data, the co-adaptive framework (Vidaurre et al. 2011), instructive framework (Jeunet et al. 2016), and merging steady-state somatosensory evoked potential and MI (Ahn et al. 2014) have been proposed, using the same stimulus timing as in online experimentation as much as possible (Cho et al. 2015).

#### 23.2.1.7.5 *MI Instructions*

Interestingly, optimal MI instruction remains unknown. Here, we adopted the imagination of complex finger movements, as shown in Figure 23.3, based on a mu rhythm tutorial in a BCI2000 workshop held in 2011 that proposed kinesthetic and visual MI (Guillot et al. 2009; Neuper et al. 2005; Stinear et al. 2006). Stinear et al. (2006) reported that kinesthetic MI modulates corticomotor excitability more than visual MI does. Furthermore, the speed of the imagined clenching has been demonstrated (Yuan et al. 2010), and recently, an instructive framework of MI has been proposed (Jeunet et al. 2016).

#### 23.2.1.7.6 *Questionnaire*

Although we have indicated already that BCI illiteracy, performance variation, and subject-to-subject transfer are complex issues, understanding subjects' metadata is also challenging, including examples such as “woman versus man,” “younger versus older,” size of head, individual personality, and so on.

### 23.2.2 TRAINING ALGORITHMS AND OFFLINE ANALYSIS

Here, we introduce the procedures for preprocessing, training the spatial filter, and selecting a classifier in BioComputing. At the end of this section, we discuss research topics with respect to preprocessing, the training feature extraction filter, and classification.

#### 23.2.2.1 **Preprocessing**

After recording MI data, we had five files (\*.dat) from the BCI2000 system because we recorded five runs, as shown in Table 23.1. BCI2000 provides a MATLAB® code, “BCI2000import.m,” to convert each \*.dat file to the EEGLab format of MATLAB. EEGLab is a well-known EEG signal processing toolbox (Delorme and Makeig 2004). In the EEGLab data structure, an “event” variable contains trigger information. The data length of each “event” variable is the same with respect to the number of stimuli. The “event” variable includes three variables: latency, position, and type.



The “latency” variable contains the time point value of a triggered stimulus within the run data. The “position” variable indicates the position of the stimulus array of the configuration in BCI2000. This value can be considered a class label, because the first and second values in our MI experiment are left- and right-hand MI instructions, as shown in Figure 23.2. Last, the “type” variable indicates the type of stimulus code. In an online experiment, there are many types of stimulus codes in BCI2000, for example, the stimulus, target, and feedback codes, and so on; then, we have raw EEG and trigger information, including latency and stimulus labels. We can extract each trial data from five runs of data. Depending on the latency of each stimulus (onset), the data frame extracted was between –2000 and 5000 ms. We carried out the same procedure for non–task-related data as well.

### 23.2.2.1.1 Offline Analysis

We checked the event-related desynchronization/synchronization (ERD/ERS) of somatosensory rhythm (SMR) for each subject (Pfurtscheller and Da Silva 1999). To calculate ERD/ERS for each channel, we followed the same procedure as did those authors using the following steps:

- Band-pass filtering of all trials at 8–30 Hz.
- Hilbert transformation of all trials.
- Taking absolute magnitude for each complex value of all trials.
- Averaging the magnitude of Hilbert transformed samples across all trials.
- We performed baseline correction for each trial to obtain percentage values for ERD/ERS

using the formula  $ERD\% = \frac{A - R}{R} \times 100$ , where  $A$  is each time sample and  $R$  is the mean value of the baseline period, which was between –500 and 0 ms.

Figure 23.4 illustrates the ERD/ERS results and shows the grand averaged ERD/ERS% over 38 subjects who had better classification rates than random chance. We plotted the topography and a bar graph of the intensive ERD period (500–2500 ms), as shown in Figure 23.4b and c. The

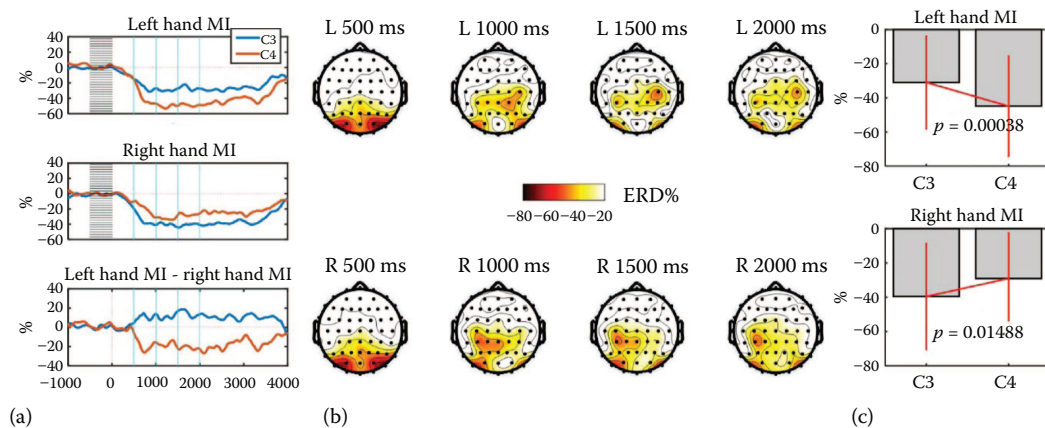


**FIGURE 23.4** ERD of SMR (8–14 Hz) from discriminative subjects (38 subjects). (a) The first and second rows show ERD of the C3 and C4 channels in left- and right-hand MI, respectively, and the last row shows the difference in ERDs between the two. The gray shaded region is the baseline period. Cyan vertical lines represent time points, such as 500, 1000, 1500, and 2000 ms. (b) Topographies of ERDs at the cyan-colored time points in (a). Initials “L” and “R” indicate left and right MI movements, respectively. (c) Comparison of ERD at C3 and C4 channels within 500–2500 ms.  $p$  values were estimated by paired  $t$  test. (Adapted from Cho, H., Ahn, M., Ahn, S., Kwon, M., and Jun, S.C., 2017. EEG datasets for motor imagery brain computer interface. *GigaScience*. DOI: <https://doi.org/10.1093/gigascience/gix034>. Copyright 2017 by GigaScience.)

topographies showed that central, parietal, and occipital areas are involved in the MI task. Bar graphs of left-hand MI show that the contralateral ERD (C4 channel) was stronger than was the ipsilateral ERD (C3 channel).

### 23.2.2.3 Feature Extraction

For the training algorithm, each trial was band-pass filtered with an 8- to 30-Hz filter and extracted temporally 500–2500 ms after the stimulus onset. The range 8–30 Hz is a well-known frequency band of the SMR or alpha and beta rhythms (Pfurtscheller and Da Silva 1999). Researchers have reported that there are individual frequency bands of SMR. It is possible to improve classification accuracy by applying individual frequency bands of SMR to train algorithms (Ang et al. 2008; Cho et al. 2012, 2015; Dornhege et al. 2006; Lemm et al. 2005; Nikulin et al. 2011; Tomioka et al. 2006). Here, we simply filtered the data spectrally with a broad band of SMR. In the temporal behavior of SMR, inhibition begins at 500 ms and is quite general for most subjects (Pfurtscheller and Da Silva 1999). Similar to the individual differences found in SMR, individual featured time windows also exist and knowing these can improve classification accuracy. However, for the simplicity of our step-by-step tutorial, we applied the same temporal window to each participant.

In the field of EEG-based MI BCI, the CSP algorithm is a very well-known and efficient method used to extract discriminative features from two different conditioned brain signals—generally, left-/right-hand MI (Blankertz et al. 2008; Fukunaga 1972; Koles 1991; Ramoser et al. 2000). The CSP algorithm finds vectors that maximize the variance for one class while simultaneously minimizing the variance for the other. The vectors are common spatial filters focused on channels that are highly effective in differentiating between the two classes. This is expressed by the following optimization problem:

$$\max_w \left( \frac{w^T C_1 w}{w^T C_2 w} \right), \quad (23.1)$$

where  $T$  denotes transpose,  $C_i$  is the spatial covariance matrix of  $X_i$  from class  $i$ , and  $X_i$  are the raw data for class  $i$  (matrix of size # of channels  $\times$  # of the time samples), assuming a zero mean for the EEG signals. This assumption is generally met when the EEG signals are band-pass filtered. The optimization problem is equivalent to this form:

$$C_1 w = \lambda C_2 w. \quad (23.2)$$

We obtained a generalized eigenvalue problem. By solving this problem, we were able to identify the filters, or the eigenvectors corresponding to the largest eigenvalues. We referred to the eigenvectors  $W$  spatial filters and  $(W^{-1})^T$  spatial patterns. Meanwhile, we are able to call filter  $W$  the de-mixing (backward model) matrix and  $(W^{-1})^T$  the mixing matrix (forward model) for time points (Blankertz et al. 2008; Parra et al. 2005). For example, if  $X$  equals the data observed (mixed data), then  $Z (=W^T X)$  is the data projected (de-mixed data or source data). Thus,  $X (= (W^{-1})^T Z)$  are mixed data with different sources in  $Z$ , and the values in the spatial filters explain which channels are important in extracting the source feature, while the values in spatial patterns explain which sources are important in generating mixed data  $X$ . When we used CSP for feature extraction, the EEG signal was projected onto the  $w$  filters. Next, we took the logarithm to the projected EEG signal variance.

As Figure 23.5 shows,  $w_1$  and  $w_2$  are the eigenvectors corresponding to the largest eigenvalue and the smallest eigenvalue obtained by solving Equation 23.2.  $w_1$  is for class 1 or left-hand MI, while  $w_2$  is for class 2 or right-hand MI. By using the “eig()” function in MATLAB, we can obtain the CSP filters easily. Here,  $w_1$  is a  $64 \times 1$ -dimensional vector because of the number of channels, as shown in Figure 23.1.  $X^{(k)}$  is the trial data in a  $64 \times 1024$  (= sampling rate  $\times$  2 s of extracted window) matrix.

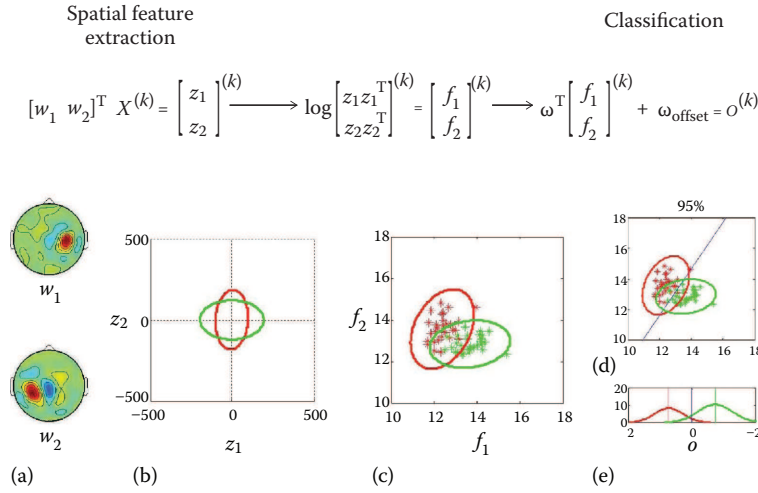


**FIGURE 23.5** Conventional CSP and FLDA model: (a) CSP filters; (b) projected signal variance: green indicates left-hand MI and red indicates right-hand MI; (c) log variance of projected feature; (d) FLDA's discrimination line; and (e) distributions of classifier outputs for two classes. (Adapted from Cho, H., Ahn, M., Kim, K., and Jun, S.C., 2015. Increasing session-to-session transfer in a brain–computer interface with on-site background noise acquisition. *Journal of Neural Engineering*, 12 (6), 66009. Copyright 2015 by the *Journal of Neural Engineering*.)

Figure 23.5a shows that the topographies of  $w_1$  and  $w_2$ .  $z_1 (= w_1^T \cdot X^{(k)})$  and  $z_2 (= w_2^T \cdot X^{(k)})$  are projected data. Figure 23.5b shows the distribution along the  $z_1$  and  $z_2$  axes. Each point in Figure 23.5b is  $(z_1(t), z_2(t))$ , where  $t$  is the time index among the 1024 time points. Figure 23.5b shows two distributions of a left MI trial and right MI data. The green distribution indicates the projected left MI  $X_1^{(k)}$ , and the red distribution indicates the projected right MI  $X_2^{(k)}$ . Each distribution was maximized to the corresponding axis.  $f_1$  and  $f_2$  are scalar values. Because the projected data are squared, the distribution of the squared values is not Gaussian. If we take the logarithm of the squared data, then the variation in large values can be reduced to obtain a Gaussian distribution. This log-variance also helps satisfy the basic assumption for FLDA, which is that two-class data have a Gaussian distribution. Therefore, the number of red stars in Figure 23.5c is equal to the number of training trials. Figure 23.5c shows the distributions of trials for left and right MI data. Finally, we can obtain the  $F_i$  matrix ( $2 \times \text{trials}$ ) for class  $i$ , where  $F = [F_i^{(1)}, F_i^{(2)}, \dots, F_i^{(N)}]$  and  $F_i^{(k)} = [f_1 f_2]^T$ .

#### 23.2.2.4 Classification

As Figure 23.5c shows, the training data  $F_i$  are prepared for classification. FLDA is a simple classifier used frequently in the BCI field and assumes that the two distributions are Gaussian. Interestingly, the objective functions of FLDA also use a Rayleigh quotient similar to the objective function of CSP, as shown in Equation 23.1. The formula of FLDA is expressed as

$$\max_{\omega} \left( \frac{\omega^T S_B \omega}{\omega^T S_w \omega} \right), \quad (23.3)$$

where  $S_B$  is  $(\mu_1 - \mu_2) \cdot (\mu_1 - \mu_2)^T$ ,  $\mu_i$  is a mean vector of data of  $F_i$  from class  $i$ , and  $S_w$  is the sum of two covariance matrices of  $F_1$  and  $F_2$ . This equation maximizes the difference between mean vectors while minimizing both covariances of the two-class data. The optimization problem can be solved as

$$S_B \omega = \lambda S_w \omega. \quad (23.4)$$

Here, we encounter a generalized eigenvalue problem again. By solving this problem, we can obtain an eigenvector  $\omega$  corresponding to the largest eigenvalue. The eigenvector  $\omega$  is the normal to the discriminant hyperplane. The  $\omega_{\text{offset}}$  can be calculated by  $\omega^T \cdot 0.5 \cdot (\mu_1 + \mu_2)$ . Finally, we can classify a trial data set by ensuring that  $\omega^T \cdot F^{(k)} + \omega_{\text{offset}} > 0$ . In Figure 23.5d, if  $\omega^T \cdot F^{(k)} + \omega_{\text{offset}} > 0$ , then the trial can be classified as right MI data.

Last, we conducted cross-validation to calculate the performance of our MI data. For each class, we divided the 100 trials of MI data into 10 subsets of 10 trials each. Seven subsets were chosen randomly and used to train CSP and FLDA, and the three subsets remaining were used to test them. This procedure was repeated 120 times by choosing 3 among the 10 subsets randomly. Finally, we estimated and averaged 120 classification accuracies.

The mean accuracy of the BCI performance over the 50 subjects, excluding bad subjects, was 67.46% ( $\pm 13.17\%$ ) in our data sets. In the BCI2000 MI data set (EEG Motor Movement/Imagery Dataset 2016; Goldberger et al. 2000; Schalk et al. 2004), the average accuracy was 60.42% ( $\pm 11.68\%$ ) over 109 subjects using CSP and FLDA. In our data sets, 14 subjects (26.92% of 52 subjects) showed low BCI performance (below chance, which is the upper confidence limit of chance with  $\alpha = 5\%$ ), as shown in Figure 23.6. This is greater than a report on 99 subjects (Guger et al. 2003) and showed that 6.7% of the subjects had accuracies lower than 60% (here, the average accuracy over the 99 subjects was not reported). Compared with the EEG Motor Movement/Imagery Dataset (2016), our data sets included more trials, although we rejected bad trials and excluded them from the results. The EEG Motor Movement/Imagery Dataset (2016) includes MI data for 109 subjects, but the number of total trials for each subject is approximately 20 trials, which has a random chance level of 65% ( $\alpha = 5\%$ ).

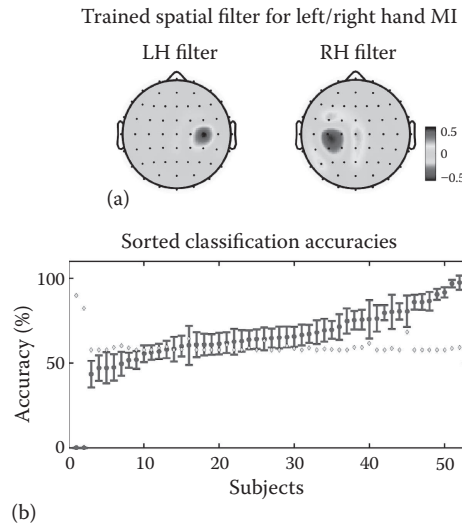


**FIGURE 23.6** Trained CSP filters for left and right hand motor imagery data and sorted cross-validated classification results. (a) To demonstrate the discriminative feature of our data set, CSP filters were trained by averaged covariance matrix of thirty-eight subjects who have high BCI performance ( $>$ random chance). (b) Sorted cross-validated classification results. Sorted accuracies are depicted in increasing order. Fourteen subjects showed low BCI performance ( $<$ chance marked with yellow diamond). Because of sorting, the number on the  $x$  axis does not correspond to subject numbers “s01” to “s52.” (Adapted from Cho, H., Ahn, M., Ahn, S., Kwon, M., and Jun, S.C., 2017. EEG datasets for motor imagery brain computer interface. *GigaScience*. DOI: <https://doi.org/10.1093/gigascience/gix034>. Copyright 2017 by GigaScience.)

### 23.2.2.5 Discussion

#### 23.2.2.5.1 Preprocessing

In any trial, various artifacts—movement-related noise, eye blinking, eye movement, heart-related noise, and so on—can contaminate the data. In this tutorial, we simply used an 8- to 30-Hz band-pass filter to remove eye-related noise above the 8-Hz earmark. To remove eye blinking or heart-related noise, an independent component analysis is a better solution than is band-pass filtering. Here, we recommend using the EEGLab MATLAB toolbox (Delorme and Makeig 2004; Wang et al. 2012). To extract reliable and stationary EEG, stationary subspace analysis (von Bünau et al. 2009) and spatio-spectral decomposition (Nikulin et al. 2011) have been proposed.

#### 23.2.2.5.2 Offline Analysis

Understanding the SMR of MI can improve hyperparameter selection for training feature extraction and classification algorithms. The  $r$ -squared analysis is a well-known method used to identify individual frequency bands (Schalk et al. 2004). In their appendix, Blankertz et al. (2008) introduced simple algorithms to identify discriminant time windows and frequency bands. To select the best frequency band, the algorithm calculates correlations between each point in a channel using a frequency matrix of MI trials and class labels. Similar to frequency band selection, the algorithm used to locate the best time window of MI calculates correlations between each point in a channel using a time matrix of absolute Hilbert transformed trial and class labels. Therefore, BCI performance can be improved using the results of offline analysis to identify individual frequency bands and time windows. In addition, the well-known offline analysis MATLAB toolboxes EEGLab (Delorme and Makeig 2004) and Fieldtrip (Oostenveld et al. 2010) can be used.

#### 23.2.2.5.3 Feature Extraction

Because of the spatial properties of left and right MI, CSP is a very powerful method. As shown in Figure 23.4, the spatial features of left MI can be observed in the right sensorimotor area, while the spatial features of right MI can be observed in the left sensorimotor area. Since CSP was first proposed approximately a decade ago, many variants of CSP algorithms have been developed, and numerous CSP ideas have been proposed to overcome session and subject variation. Representatively, regularized CSP theory adopts two approaches to regularize the CSP algorithm: regularizing covariance matrix and the objective function of CSP (Lotte and Guan 2011). Furthermore, expanding the spatio-spectral feature space also can improve BCI performance with respect to session and subject variation.

#### 23.2.2.5.4 Classification

A review of classification methods for BCI (Lotte et al. 2007) showed that a support vector machine (SVM) was the best classifier among the existing algorithms. Compared with FLDA, SVM is a successful system to classify outliers and therefore is a more universal classifier than is FLDA. Previously, there were few studies that addressed the deep neural network (Sakhavi et al. 2015; Walker et al. 2015). However, a recent study of this topic showed compelling results. DNN accomplishes both feature extraction and classification in one structure. To achieve improved BCI performance, the DNN approach requires more investigation of its hyperparameters (optimal number of layers, activation functions, etc.) and weights analysis. After the training DNN, what is the meaning of weights in the layers with respect to signal processing?

## 23.3 TESTING SESSION

### 23.3.1 ONLINE EXPERIMENT

In any testing session, the method used to classify new data largely is the same as that used in training sessions. New data were processed every 2 s in our testing sessions. A trial of the online experimental paradigm implemented by the BCI2000 system is shown in Figure 23.7. We used the



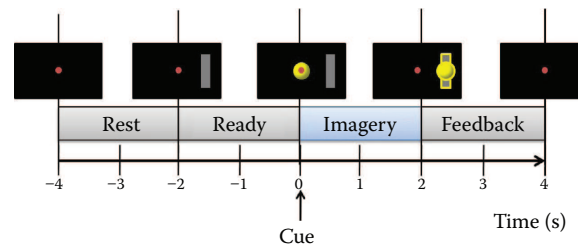


**FIGURE 23.7** Online experimental paradigm. The yellow ball is controlled by the data collected from 0 to 2 s after the cue (blue). The red point on the screen was the fixation point. (Adapted from Cho, H., Ahn, M., Kim, K., and Jun, S.C., 2015. Increasing session-to-session transfer in a brain–computer interface with on-site background noise acquisition. *Journal of Neural Engineering*, 12 (6), 66009. Copyright 2015 by the *Journal of Neural Engineering*.)

Biosemi acquisition module for signal acquisition and adopted the MATLAB signal processing module to load trained weights of CSP and FDLA and to classify the new data in real time. The application module was a cursor task application with a 2-s sliding window. After the 2-s rest, 2 s of MI instruction were shown as a gray bar. Following this instruction, the subject conducted left- or right-hand MI. If a gray bar appeared on the right side, then the subject was supposed to imagine right-hand finger movements. This 2-s period was classified by trained CSP and FLDA in the MATLAB signal processing module, and the classified result was transmitted to the cursor task application. Finally, after the 2-s imagination period, the cursor was moved according to the classified result, as shown in Figure 23.7. These new data were band-pass filtered at 8–30 Hz, filtered spatially by CSP, and the feature extracted was classified by FLDA, as shown in Figure 23.5. Here, the size of the sliding window was 2 s because it was the period used in the training session.

### 23.3.2 DISCUSSION

Representatively, BCI2000 (Schalk et al. 2004) and OpenVibe (Renard et al. 2010) are recommended for online BCI feedback. For BCI beginners, OpenVibe is easy to use because it supports graphical language. However, based on our experience, because of the graphical language, OpenVibe requires relatively large memory spaces. Thus, the BCI2000 system is lighter than is OpenVibe.

A limitation of our online experiment was a mismatch between the time windows featured. While the training session time window was 500–2500 ms after onset, the time window of the classified new data was 0–2000 ms. To overcome this mismatch problem, we applied an online experimental paradigm used in training sessions in other work (Cho et al. 2015). For MI data classification, it is very important to extract the most discriminative time window for offline data in training algorithms. The online experimental paradigm in this chapter was included in synchronous BCI, which has trial and stimulus cues. For asynchronous BCI, which has no instruction onset or cue, recognizing the user's self-cues is also challenging, for example, classifying the resting and task states.

To minimize the gap between training and testing sessions, BCI researchers have proposed adaptive and co-adaptive approaches (Baldwin and Penaranda 2012; Satti et al. 2010; Shenoy et al. 2006; Shin et al. 2015; Sun and Zhang 2006; Vidaurre et al. 2011). Here, “adaptive” means “let the machine learn in real time” and “co-adaptive” means “let both the user and machine learn.” In the adaptive approach, either CSP or FLDA was updated with new data after each online trial. Controlling the learning rate or gradient was challenging. The co-adaptive approach showed improved BCI performance and a possible solution to BCI illiteracy. Furthermore, there are additional reasons for the gap between training and testing sessions, including psychological and environmental differences, among others. Thus, minimizing the gap between training and testing sessions remains a difficult issue to resolve.

A particular missing point in the training session section was the information transfer rate (ITR), which provides a general assessment of BCI performance. Actually, ITR is a critical feature of MI

BCI with respect to human–computer interaction. At the beginning of BCI research, many people were interested in BCI because it can provide a new communication channel without any limb movement; however, the ITR in BCI is much lower than that in other input interfaces, including keyboard, mouse, and joystick. Very few studies (Bin et al. 2011; Wang et al. 2008) have shown an ITR that exceeds 100 bits/min (not based on MI). For comparison, the ITRs using a keyboard or mouse are 900 bits/min and a few hundred bits per minute, respectively (Clerc et al. 2016). If a BCI could somehow demonstrate a rate similar to that of keyboard use, that would be highly innovative.

## 23.4 SUMMARY

In this chapter, we provided a step-by-step tutorial for MI BCI and discussed research topics related to each step. In the training sessions, we detailed recording data issues, including software, device, environment, experimental paradigm, MI instruction, and questionnaire, offline analysis, and training algorithms. In the testing session, we introduced a simple procedure of cursor task application and discussed time window and synchronous/asynchronous issues.

We not only provided a step-by-step tutorial but also discussed possible ways to improve the data quality and MI BCI performance. We selected the most promising, yet challenging issues, as follows: recording device, experimental paradigm or MI instruction, metadata analysis for subject/session variation or BCI illiteracy, DNN, asynchronous MI BCI, and ITR. BCI researchers have made tremendous efforts to resolve these challenging issues. Thus, it is our hope that more innovative and easy-to-use BCI will be developed in the near future.

## ACKNOWLEDGMENTS

This work was supported by Institute for Information and Communications Technology Promotion (IITP) grant funded by the Korean government (No. 2017-0-00451) and Ministry of Culture, Sports and Tourism (MCST) and Korea Creative Content Agency (KOCCA) in the Culture Technology (CT) Research and Development Program 2017.

## REFERENCES

- Ahn, M., Cho, H., Ahn, S., and Jun, S.C., 2013. High theta and low alpha powers may be indicative of BCI-illiteracy in motor imagery. *PloS one*, 8 (11), e80886.
- Ahn, M. and Jun, S.C., 2015. Performance variation in motor imagery brain–computer interface: A brief review. *Journal of Neuroscience Methods*, 243, 103–110.
- Ahn, S., Ahn, M., Cho, H., and Jun, S.C., 2014. Achieving a hybrid brain–computer interface with tactile selective attention and motor imagery. *Journal of Neural Engineering*, 11 (6), 66004.
- Ahn, S., Nguyen, T., Jang, H., Kim, J.G., and Jun, S.C., 2016. Exploring neuro-physiological correlates of drivers' mental fatigue caused by sleep deprivation using simultaneous EEG, ECG, and fNIRS data. *Frontiers in Human Neuroscience*, 10.
- Ang, K.K., Chin, Z.Y., Zhang, H., and Guan, C., 2008. Filter bank common spatial pattern (FBCSP) in brain–computer interface. In: *Neural Networks, 2008. IJCNN 2008 (IEEE World Congress on Computational Intelligence)*. *IEEE International Joint Conference on*. IEEE, 2390–2397.
- Baldwin, C.L. and Penaranda, B.N., 2012. Adaptive training using an artificial neural network and EEG metrics for within-and cross-task workload classification. *NeuroImage*, 59 (1), 48–56.
- Besio, G., Koka, K., Aakula, R., and Dai, W., 2006. Tri-polar concentric ring electrode development for Laplacian electroencephalography. *IEEE Transactions on Biomedical Engineering*, 53 (5), 926–933.
- Bin, G., Gao, X., Wang, Y., Li, Y., Hong, B., and Gao, S., 2011. A high-speed BCI based on code modulation VEP. *Journal of Neural Engineering*, 8 (2), 25015.
- Blankertz, B., Dornhege, G., Krauledat, M., Müller, K.-R., Kunzmann, V., Losch, F., and Curio, G., 2006. The Berlin Brain–Computer Interface: EEG-based communication without subject training. *IEEE Transactions on Neural Systems and Rehabilitation Engineering*, 14 (2), 147–152.
- Blankertz, B., Sannelli, C., Halder, S., Hammer, E.M., Kübler, A., Müller, K.-R., Curio, G., and Dickhaus, T., 2010. Neurophysiological predictor of SMR-based BCI performance. *Neuroimage*, 51 (4), 1303–1309.

- Blankertz, B., Tomioka, R., Lemm, S., Kawanabe, M., and Muller, K.-R., 2008. Optimizing spatial filters for robust EEG single-trial analysis. *IEEE Signal Processing Magazine*, 25 (1), 41–56.
- von Büna, P., Meinecke, F.C., and Müller, K.-R., 2009. Stationary subspace analysis. In: *International Conference on Independent Component Analysis and Signal Separation*. Springer, 1–8.
- Cho, H., Ahn, M., Ahn, S., and Jun, S.C., 2012. Invariant common spatio-spectral patterns. In: *Proc. of TOBI 3rd Workshop*. 31–32.
- Cho, H., Ahn, M., Ahn, S., Kwon, M., and Jun, S.C., 2017. EEG datasets for motor imagery brain computer interface. *GigaScience*. DOI: <https://doi.org/10.1093/gigascience/gix034>
- Cho, H., Ahn, M., Kim, K., and Jun, S.C., 2015. Increasing session-to-session transfer in a brain–computer interface with on-site background noise acquisition. *Journal of Neural Engineering*, 12 (6), 66009.
- Cincotti, F., Bianchi, L., Birch, G., Guger, C., Mellinger, J., Scherer, R., Schmidt, R.N., Suárez, O.Y., and Schalk, G., 2006. BCI Meeting 2005—Workshop on technology: Hardware and software. *IEEE Transactions on Neural Systems and Rehabilitation Engineering*, 14 (2), 128–131.
- Clerc, M., Bougrain, L., and Lotte, F., 2016. *Brain–Computer Interfaces 1: Methods and Perspectives*. John Wiley & Sons.
- Delorme, A. and Makeig, S., 2004. EEGLAB: An open source toolbox for analysis of single-trial EEG dynamics including independent component analysis. *Journal of Neuroscience Methods*, 134 (1), 9–21.
- Dornhege, G., Blankertz, B., Krauledat, M., Losch, F., Curio, G., and Muller, K.-R., 2006. Combined optimization of spatial and temporal filters for improving brain–computer interfacing. *IEEE Transactions on Biomedical Engineering*, 53 (11), 2274–2281.
- EEG Motor Movement/Imagery Dataset [online], 2016. Available from: <https://physionet.org/pn4/eegmmidb/> [Accessed 20 Dec 2016].
- Fazli, S., Popescu, F., Danóczy, M., Blankertz, B., Müller, K.-R., and Grozea, C., 2009. Subject-independent mental state classification in single trials. *Neural Networks*, 22 (9), 1305–1312.
- Fukunaga, K., 1972. *Introduction to Statistical Pattern Recognition*. Academic Press.
- Goldberger, A.L., Amaral, L.A.N., Glass, L., Hausdorff, J.M., Ivanov, P.C., Mark, R.G., Mietus, J.E., Moody, G.B., Peng, C.-K., and Stanley, H.E., 2000. PhysioBank, PhysioToolkit, and PhysioNet. *Circulation*, 101 (23), e215–e220.
- Guger, C., Edlinger, G., Harkam, W., Niedermayer, I., and Pfurtscheller, G., 2003. How many people are able to operate an EEG-based brain–computer interface (BCI)? *IEEE Transactions on Neural Systems and Rehabilitation Engineering*, 11 (2), 145–147.
- Guillot, A., Collet, C., Nguyen, V.A., Malouin, F., Richards, C., and Doyon, J., 2009. Brain activity during visual versus kinesthetic imagery: An fMRI study. *Human Brain Mapping*, 30 (7), 2157–2172.
- Jeunet, C., Jahanpour, E., and Lotte, F., 2016. Why standard brain–computer interface (BCI) training protocols should be changed: An experimental study. *Journal of Neural Engineering*, 13 (3), 36024.
- Koles, Z.J., 1991. The quantitative extraction and topographic mapping of the abnormal components in the clinical EEG. *Electroencephalography and Clinical Neurophysiology*, 79 (6), 440–447.
- Kothe, C.A. and Makeig, S., 2013. BCILAB: A platform for brain–computer interface development. *Journal of Neural Engineering*, 10 (5), 56014.
- Lemm, S., Blankertz, B., Curio, G., and Muller, K.-R., 2005. Spatio-spectral filters for improving the classification of single trial EEG. *IEEE Transactions on Biomedical Engineering*, 52 (9), 1541–1548.
- Lotte, F., Congedo, M., Lécuyer, A., Lamarche, F., and Arnaldi, B., 2007. A review of classification algorithms for EEG-based brain–computer interfaces. *Journal of Neural Engineering*, 4 (2), R1.
- Lotte, F., Guan, C., and Ang, K.K., 2009. Comparison of designs towards a subject-independent brain–computer interface based on motor imagery. In: *2009 Annual International Conference of the IEEE Engineering in Medicine and Biology Society*. IEEE, 4543–4546.
- Lotte, F. and Guan, C., 2011. Regularizing common spatial patterns to improve BCI designs: unified theory and new algorithms. *IEEE Transactions on Biomedical Engineering*, 58 (2), 355–362.
- Mattia, D., Astolfi, L., Toppi, J., Petti, M., Pichiorri, F., and Cincotti, F., 2016. Interfacing brain and computer in neurorehabilitation. In: *Brain–Computer Interface (BCI), 2016 4th International Winter Conference on*. IEEE, 1–2.
- Neuper, C., Scherer, R., Reiner, M., and Pfurtscheller, G., 2005. Imagery of motor actions: Differential effects of kinesthetic and visual–motor mode of imagery in single-trial EEG. *Cognitive Brain Research*, 25 (3), 668–677.
- Nguyen, T., Ahn, S., Jang, H., Jun, S.C., and Kim, J.G., 2016. Applying support vector machine on hybrid fNIRS/EEG signal to classify driver's conditions (Conference Presentation). In: *SPIE BiOS*. International Society for Optics and Photonics, 969003–969003.
- Nikulin, V.V., Nolte, G., and Curio, G., 2011. A novel method for reliable and fast extraction of neuronal EEG/MEG oscillations on the basis of spatio-spectral decomposition. *NeuroImage*, 55 (4), 1528–1535.



- Oostenveld, R., Fries, P., Maris, E., and Schoffelen, J.-M., 2010. FieldTrip: Open Source Software for Advanced Analysis of MEG, EEG, and Invasive Electrophysiological Data. *Computational Intelligence and Neuroscience*, 2011, e156869.
- Parra, L.C., Spence, C.D., Gerson, A.D., and Sajda, P., 2005. Recipes for the linear analysis of EEG. *Neuroimage*, 28 (2), 326–341.
- Pfurtscheller, G. and Da Silva, F.L., 1999. Event-related EEG/MEG synchronization and desynchronization: basic principles. *Clinical Neurophysiology*, 110 (11), 1842–1857.
- Pichiorri, F., Morone, G., Petti, M., Toppi, J., Pisotta, I., Molinari, M., Paolucci, S., Inghilleri, M., Astolfi, L., Cincotti, F., and others, 2015. Brain–computer interface boosts motor imagery practice during stroke recovery. *Annals of Neurology*, 77 (5), 851–865.
- Ramoser, H., Muller-Gerking, J., and Pfurtscheller, G., 2000. Optimal spatial filtering of single trial EEG during imagined hand movement. *IEEE Transactions on Rehabilitation Engineering*, 8 (4), 441–446.
- Renard, Y., Lotte, F., Gibert, G., Congedo, M., Maby, E., Delannoy, V., Bertrand, O., and Lécuyer, A., 2010. Openvibe: An open-source software platform to design, test, and use brain–computer interfaces in real and virtual environments. *Presence: Teleoperators and Virtual Environments*, 19 (1), 35–53.
- Reuderink, B., Farquhar, J., Poel, M., and Nijholt, A., 2011. A subject-independent brain–computer interface based on smoothed, second-order baselining. In: *2011 Annual International Conference of the IEEE Engineering in Medicine and Biology Society*. IEEE, 4600–4604.
- Sakhavi, S., Guan, C., and Yan, S., 2015. Parallel convolutional-linear neural network for motor imagery classification. In: *Signal Processing Conference (EUSIPCO), 2015 23rd European*. IEEE, 2736–2740.
- Samek, W., Meinecke, F.C., and Müller, K.R., 2013. Transferring subspaces between subjects in brain–computer interfacing. *IEEE Transactions on Biomedical Engineering*, 60 (8), 2289–2298.
- Satti, A., Guan, C., Coyle, D., and Prasad, G., 2010. A covariate shift minimisation method to alleviate non-stationarity effects for an adaptive brain–computer interface. In: *Pattern Recognition (ICPR), 2010 20th International Conference on*. IEEE, 105–108.
- Schalk, G., McFarland, D.J., Hinterberger, T., Birbaumer, N., and Wolpaw, J.R., 2004. BCI2000: A general-purpose brain–computer interface (BCI) system. *IEEE Transactions on Biomedical Engineering*, 51 (6), 1034–1043.
- Shenoy, P., Krauledat, M., Blankertz, B., Rao, R.P.N., and Müller, K.-R., 2006. Towards adaptive classification for BCI. *Journal of Neural Engineering*, 3 (1), R13.
- Shin, Y., Lee, S., Ahn, M., Cho, H., Jun, S.C., and Lee, H.-N., 2015. Simple adaptive sparse representation based classification schemes for EEG based brain–computer interface applications. *Computers in Biology and Medicine*, 66, 29–38.
- Stinear, C.M., Byblow, W.D., Steyvers, M., Levin, O., and Swinnen, S.P., 2006. Kinesthetic, but not visual, motor imagery modulates corticomotor excitability. *Experimental Brain Research*, 168 (1–2), 157–164.
- Sun, S. and Zhang, C., 2006. Adaptive feature extraction for EEG signal classification. *Medical and Biological Engineering and Computing*, 44 (10), 931–935.
- Tomioka, R., Dornhege, G., Nolte, G., Blankertz, B., Aihara, K., and Müller, K.-R., 2006. Spectrally weighted common spatial pattern algorithm for single trial EEG classification. *Dept. Math. Eng., Univ. Tokyo, Tokyo, Japan, Tech. Rep.*, 40.
- Tu, W. and Sun, S., 2012. A subject transfer framework for EEG classification. *Neurocomputing*, 82, 109–116.
- Vidaurre, C., Sannelli, C., Müller, K.-R., and Blankertz, B., 2011. Co-adaptive calibration to improve BCI efficiency. *Journal of Neural Engineering*, 8 (2), 25009.
- Walker, I., Deisenroth, M., and Faisal, A., 2015. Deep convolutional neural networks for brain computer interface using motor imagery. *Imperial College of Science, Technology and Medicine Department of Computing*.
- Wang, Y., Gao, X., Hong, B., Jia, C., and Gao, S., 2008. Brain–computer interfaces based on visual evoked potentials. *IEEE Engineering in Medicine and Biology Magazine*, 27 (5).
- Wang, Y., Wang, Y.-T., and Jung, T.-P., 2012. Translation of EEG spatial filters from resting to motor imagery using independent component analysis. *PloS one*, 7 (5), e37665.
- Wolpaw, J. and Wolpaw, E.W., 2012. *Brain–Computer Interfaces: Principles and Practice*. OUP USA.
- Wolpaw, J.R., McFarland, D.J., Neat, G.W., and Forneris, C.A., 1991. An EEG-based brain–computer interface for cursor control. *Electroencephalography and Clinical Neurophysiology*, 78 (3), 252–259.
- Yuan, H., Perdoni, C., and He, B., 2010. Relationship between speed and EEG activity during imagined and executed hand movements. *Journal of Neural Engineering*, 7 (2), 26001.